Interaction of charged particles with surface plasmons in cylindrical channels in solids

Néstor R. Arista and Miguel A. Fuentes
Instituto Balseiro and Centro Atómico Bariloche, Comisión Nacional de Energía Atómica, 8400 S.C. Bariloche, Argentina
(Received 11 September 2000; published 27 March 2001)

The interaction between swift charged particles and the electronic surface modes of a cylindrical cavity is described according to classical and quantum-mechanical formulations. We perform a quantization of the collective modes and obtain expressions for the coupling with external probes moving with arbitrary trajectories. We study the case of particles moving parallel to the channel axis and derive the probabilities of single and multiple plasmon excitation and the average energy loss. A correspondence between the classical and quantum pictures is shown. The scaling properties of the interaction terms are studied and general scaling functions are obtained, which may be applied to a wide range of particle velocities and cavity sizes, including microcapillaries and nanotubes.

DOI: 10.1103/PhysRevB.63.165401 PACS number(s): 79.20.Rf, 34.50.Bw, 34.50.Dy

I. INTRODUCTION

The interaction of swift ionized particles with surface-plasmon modes has become an ever-increasing part of surface physics and related studies since the pioneering work by Ritchie in 1957.[1] These modes are localized collective electronic oscillations that can be excited by charged particles or electromagnetic radiation and give place to a wide field of interesting phenomena. The quantal properties of surface plasmons have already been investigated by several workers for the case of plane surfaces or interfaces.[2–4]

In experiments with electrons, the excitation of surface plasmons may be studied through the analysis of the multiple energy-loss peaks that appear in the spectrum of the inelastically reflected particles.[5,6] Previous experiments of plasmon excitation in aloof scattering during transmission through micropores in thin metal foils (with channel radii of 20–200 nm) have also been reported,[7,8] and several theoretical studies dealing with the energy loss of charged particles in cylindrical cavities have been published.[9–11] In these papers, the energy-loss process has been described in a classical way, but the importance of the underlying mechanism of surface-plasmon excitation may be inferred from the results.

More recently, the synthesis of nanotubes of graphite or fullerenes has been reported,[12,13] and there are already electron-spectroscopy experiments.[14] and studies of particle channeling in these structures.[15], which may have small diameters of about 14 Å .[16] In addition, there is also growing interest in studying the interaction of swift ions and the formation of hollow atoms in microcapillaries and nanotubes.[17,18] Hence, the study of plasmon excitation in these systems is a subject of great current interest.

We consider in this paper the interaction between nonrelativistic charged particles and the surface modes of a cylindrical cavity using both classical and quantum-mechanical formalisms. The classical approach follows the lines of previous studies and provides a convenient link with the quantum description. The quantum formulation is derived starting from a quantization of the surface modes in order to obtain the forms of the Hamiltonians corresponding to the free collective modes and their interaction with external probes moving with arbitrary trajectories. We obtain the probabilities of single and multiple plasmon excitation and the average energy loss for particles moving parallel to the channel axis. The correspondence between the classical and quantum pictures is shown. Finally, we study the scaling properties of the interaction terms and provide general scaling functions that may be applied to describe the excitation processes for a wide range of cavity radii and particle velocities.

II. CAPILLARY MODES

The electrostatic modes of a cylindrical cavity of radius a in a solid are determined by the solutions of the Laplace equation, in terms of cylindrical Bessel functions $I_m(x)$ and $K_m(x)$, with $m=0,\pm1,\pm2,\pm3,\ldots$, as follows:[19]

(a) For $\rho<a$,

$$\phi^{(1)}=A_m e^{i(kz+m\varphi)}I_m(k\rho)e^{-i\omega t}; \tag{1}$$

(b) for $\rho>a$,

$$\phi^{(2)}=B_m e^{i(kz+m\varphi)}K_m(k\rho)e^{-i\omega t}, \tag{2}$$

where we use cylindrical coordinates (ρ,φ,z) and k is a wave vector along the axial channel direction denoted by z. The relation between the coefficients A_m and B_m, and the frequencies of the modes $\omega_{k,m}=\omega_m(k)$ may be determined by the usual matching conditions at $\rho=a$, namely $\phi^{(1)}(\rho,\varphi,z)|_{\rho=a}=\phi^{(2)}(\rho,\varphi,z)|_{\rho=a}$ and $\nabla_\rho\phi^{(1)}(\rho,\varphi,z)|_{\rho=a}=\varepsilon(\omega)\nabla_\rho\phi^{(2)}(\rho,\varphi,z)|_{\rho=a}$, where $\varepsilon(\omega)$ is the dielectric function of the medium.

This yields

$$\frac{A_m}{B_m}=\frac{K_m(ka)}{I_m(ka)} \tag{3}$$

and

$$\varepsilon(\omega)=\frac{I'_m(ka)}{I_m(ka)}\frac{K_m(ka)}{K'_m(ka)}, \tag{4}$$

where $I'_m(x)=dI_m(x)/dx$, $K'_m(x)=dK_m(x)/dx$.

Equation (4) gives implicitly the *dispersion relation* of the modes, $\omega=\omega_m(k)$. It may be solved for each material using

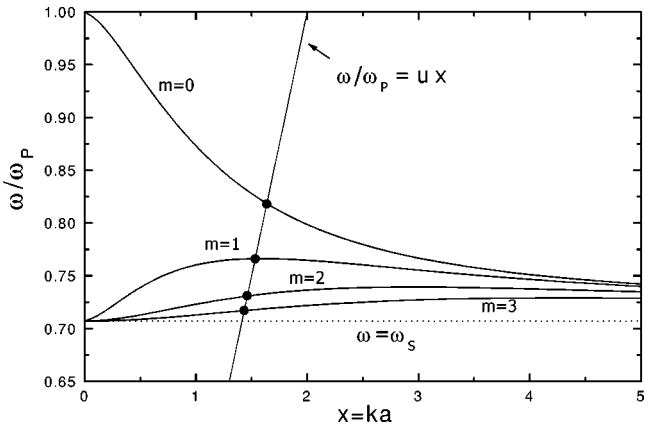

FIG. 1. Dispersion relation of the surface-plasmon modes of a cylindrical cavity $\omega_{k,m}/\omega_P$, for $m=0$, 1, 2, and 3, vs the variable $x=ka$. Some characteristic limits should be noted: for $ka\to 0$, we get $\omega_{k,m}\to\omega_P$ for $m=0$ and $\omega_{k,m}\to\omega_s$ for $m\neq 0$, whereas for $ka\to\infty$, one gets $\omega_{k,m}\to\omega_s$, where $\omega_s=\omega_P/\sqrt{2}$ is the surface-plasmon frequency corresponding to flat surfaces ($a\to\infty$ limit). The intersections of the various curves with the line $\omega/\omega_P=ux$ (solid circles) yield the conditions for the resonant excitation of each of the modes (the line $\omega/\omega_P=ux$ shown here corresponds to a reduced velocity $u=0.5$).

the appropriate expression for $\varepsilon(\omega)$. In particular, we will approximate here the dielectric function around the plasma resonance by $\varepsilon(\omega)=1-\omega_P^2/\omega(\omega+i\gamma)$, where ω_P is the plasma frequency and γ the damping constant. For $\gamma\ll\omega_P$, we obtain the frequency of the modes $\omega_{k,m}\equiv\omega_m(k)$ in the form

$$\omega_{k,m}=\frac{\omega_P}{\sqrt{1+\sigma_m(ka)}}, \tag{5}$$

where $\sigma_m(x)=-I_m'(x)K_m(x)/I_m(x)K_m'(x)$ [note that $\sigma_m(x)$ is a positive quantity since $K_m'(ka)<0$].

Using the Wronskian property[20] $I_m(x)K_m'(x)-I_m'(x)K_m(x)=-1/x$, we can write this relation in a very simple form,

$$\omega_{k,m}^2=\omega_P^2 x I_m(x)|K_m'(x)|=\omega_P^2 g_m(x), \tag{6}$$

with $x=ka$ and where we introduced the function $g_m(x)\equiv xI_m(x)|K_m'(x)|$, which has the following limits: $g_m(x)\to 1$ for $x\to 0$; $g_m(x)\to\frac{1}{2}$ for $x\to\infty$.

This shows a general scaling property of $\omega_{k,m}/\omega_P$ in terms of the variable $x=ka$. The dispersion curves for $m=0,1,2,3$ are shown in Fig. 1. Two important limits should be noted: for $ka\to 0$, we get $\omega_{k,m}\to\omega_P$ for $m=0$ (this corresponds to bulk-plasmon modes in homogeneous systems) and $\omega_{k,m}\to\omega_s$ for $m\neq 0$, whereas for $ka\to\infty$, one gets $\omega_{k,m}\to\omega_s$ in all cases, where $\omega_s=\omega_P/\sqrt{2}$ is the surface-plasmon frequency corresponding to flat surfaces ($a\to\infty$ limit).[1]

III. CLASSICAL TREATMENT

A. Field of external charge

The Coulomb potential of a charge Ze moving uniformly with trajectory parallel to the z axis, with velocity v and with instantaneous coordinates $\mathbf{x}_0=(\rho_0,\phi_0,vt)$, may be expanded in terms of cylindrical functions as follows:[19]

$$\begin{aligned}\phi_0(\rho,\phi,z,t)&=\frac{Ze}{|\mathbf{x}-\mathbf{x}_0|}\\&=\frac{2}{\pi}Ze\sum_{m=-\infty}^{\infty}\\&\quad\times\int_0^\infty dk\exp[im(\phi-\phi_0)]\\&\quad\times\cos[k(z-vt)]I_m(k\rho_<)K_m(k\rho_>).\end{aligned} \tag{7}$$

We introduce here a Fourier transform of the time coordinate, defined by

$$F(\omega)=\int_{-\infty}^{\infty}dt\,e^{i\omega t}F(t), \tag{8}$$

and obtain

$$\begin{aligned}\phi_0(\rho,\phi,z,\omega)&=2Ze\sum_{m=-\infty}^{\infty}\int_0^\infty dk\exp[im(\phi-\phi_0)]\\&\quad\times I_m(k\rho_<)K_m(k\rho_>)\\&\quad\times\{\exp(ikz)\delta(\omega-kv)\\&\quad+\exp(-ikz)\delta(\omega+kv)\}.\end{aligned} \tag{9}$$

B. Induced potential

Following the form of the external potential, Eq. (9), the induced potential inside and outside the cavity may be expanded also in a convenient way in terms of the regular solutions in each domain.

(a) $\rho<a$. Following Eq. (9), we write the induced potential as follows:

$$\begin{aligned}\phi_{ind}^{(a)}(\rho,\phi,z,\omega)&=2Ze\sum_{m=-\infty}^{\infty}\int_0^\infty dk\exp[im(\phi-\phi_0)]\\&\quad\times A_m I_m(k\rho)[\exp(ikz)\delta(\omega-kv)\\&\quad+\exp(-ikz)\delta(\omega+kv)]\end{aligned} \tag{10}$$

so that the total potential for $\rho<a$ becomes

$$\phi_{\rm tot}^{(a)}(\rho,\phi,z,\omega)=\phi_0(\rho,\phi,z,\omega)+\phi_{\rm ind}^{(a)}(\rho,\phi,z,\omega). \tag{11}$$

(b) $\rho>a$. In this case it becomes convenient to expand the total (external plus induced) potential as follows:

$$\phi^{(b)}_{\rm tot}(\rho,\phi,z,\omega)=2Ze\sum_{m=-\infty}^{\infty}\int_0^{\infty}dk\,\exp[im(\phi-\phi_0)]\times B_m K_m(k\rho)[\exp(ikz)\,\delta(\omega-kv)+\exp(-ikz)\,\delta(\omega+kv)]. \quad (12)$$

The coefficients A_m and B_m in Eqs. (10) and (12) will be determined from the boundary conditions.

C. Boundary conditions

Using the former expressions of Eqs. (9)–(12), we apply the usual matching conditions at $\rho=a$, namely

$$\phi_0(a,\phi,z,\omega)+\phi^{(a)}_{\rm ind}(a,\phi,z,\omega)=\phi^{(b)}_{\rm tot}(a,\phi,z,\omega) \quad (13)$$

and

$$\phi_0'(a,\phi,z,\omega)+\phi^{(a)'}_{\rm ind}(a,\phi,z,\omega)=\varepsilon(\omega)\phi^{(b)'}_{\rm tot}(a,\phi,z,\omega), \quad (14)$$

where the primes denote the derivatives with respect to the variable ρ.

This yields the following equations to determine the coefficients A_m and B_m:

$$I_m(k\rho_0)K_m(ka)+A_mI_m(ka)=B_mK_m(ka),$$

$$I_m(k\rho_0)K_m'(ka)+A_mI_m'(ka)=B_mK_m'(ka)\varepsilon(\omega), \quad (15)$$

and we obtain the solutions in the form $A_m(k,\omega)=I_m(k\rho_0)\tilde{A}_m(k,\omega)$, $B_m(k,\omega)=I_m(k\rho_0)\tilde{B}_m(k,\omega)$, where $\tilde{A}_m$ and $\tilde{B}_m$ are given by

$$\tilde{A}_m(k,\omega)=\frac{[1-\varepsilon(\omega)]K_m(ka)K_m'(ka)}{\varepsilon(\omega)I_m(ka)K_m'(ka)-K_m(ka)I_m'(ka)}, \quad (16)$$

$$\tilde{B}_m(k,\omega)=\frac{I_m(ka)K_m'(ka)-K_m(ka)I_m'(ka)}{\varepsilon(\omega)I_m(ka)K_m'(ka)-K_m(ka)I_m'(ka)}. \quad (17)$$

In the following, the primes in the expressions $I_m'(x)$ and $K_m'(x)$ will denote the derivatives with respect to the argument $x=ka$.

Using Eq. (16) and Fourier transforming Eq. (10), we obtain the induced potential inside the cylinder,

$$\phi^{(a)}_{\rm ind}(\rho,\phi,z,t)=2Ze\int_{-\infty}^{\infty}\frac{d\omega}{2\pi}e^{-i\omega t}\times\sum_{m=-\infty}^{\infty}\int_0^{\infty}dk\,I_m(k\rho)I_m(k\rho_0)\times e^{im(\phi-\phi_0)}\tilde{A}_m(k,\omega)[\exp(ikz)\,\delta(\omega-kv)+\exp(-ikz)\,\delta(\omega+kv)], \quad (18)$$

which, after integrating in ω, may be written as follows:

$$\phi^{(a)}_{\rm ind}(\rho,\phi,z,t)=\frac{2}{\pi}Ze\sum_{m=-\infty}^{\infty}\int_0^{\infty}dkI_m(k\rho)I_m(k\rho_0)e^{im(\phi-\phi_0)}\times\{{\rm Re}[\tilde{A}_m(k,\omega)]\cos(kz-\omega t)-{\rm Im}[\tilde{A}_m(k,\omega)]\sin(kz-\omega t)\}|_{\omega=kv}, \quad (19)$$

where we have used the property

$$\tilde{A}_m(k,\omega)+\tilde{A}_m(k,-\omega)=2\,{\rm Re}[\tilde{A}_m(k,\omega)],$$

$$\tilde{A}_m(k,\omega)-\tilde{A}_m(k,-\omega)=2i\,{\rm Im}[\tilde{A}_m(k,\omega)],$$

and the frequency is now given by $\omega=kv$.

A further useful expression for $\tilde{A}_m(k,\omega)$ that applies to the previously introduced dielectric function is the following:

$$\tilde{A}_m(k,\omega)=\frac{\omega_{k,m}^2}{\omega(\omega+i\gamma)-\omega_{k,m}^2}\frac{K_m(x)}{I_m(x)}=\frac{g_m(x)}{\Omega(\Omega+i\Gamma)-g_m(x)}\frac{K_m(x)}{I_m(x)}, \quad (20)$$

where $\Omega(x)=\omega/\omega_P=kv/\omega_P=ux$, with $u=v/\omega_Pa$ (reduced velocity), $\Gamma=\gamma/\omega_P$ and $g_m(x)\equiv xI_m(x)|K_m'(x)|$. This shows that the values of $\tilde{A}_m(k,\omega)$ may also be parametrized in a general way using reduced variables, in terms of $x=ka$.

D. Resonant excitations

According to Eq. (19), the induced field consists of a superposition of wave components that satisfy the condition $\omega=kv$. This means that only waves with phase velocities ω/k coincident with the particle velocity v will be excited by the particle. This corresponds to conditions of coherent excitation of the modes.

Then, the values of k and ω_m must be determined for each velocity v by solving the equation $\omega_m(k)=kv$. This condition is illustrated in Fig. 1 by the line $\omega/\omega_P=kv/\omega_P=ux$, with $u=v/\omega_Pa$ and $x=ka$. The values of k and ω to be used in the evaluation are those corresponding to the intersection of the line $\omega/\omega_P=ux$ with the corresponding dispersion-relation curve for each mode m. In these conditions, we have *resonant excitations*. These values are indicated by solid circles in Fig. 1 In this way, k and ω become velocity-dependent functions: $k=k_m[v]$, $\omega=\omega_m[v]$.

It may be shown that the form of the induced potential, Eq. (19), has a typical ''wake'' structure, characterized by a function of ρ and $z-vt$, which remains stationary in a frame of reference moving together with the particle at velocity v (the phenomenon of a wake potential has been studied extensively for particles moving in *homogeneous* media).[21]

IV. STOPPING FORCE ON THE PARTICLE

The potential inside and outside the capillary is given by Eqs. (10)–(12). In order to calculate the stopping force due to the induced reaction of the medium on the moving par-

ticle, it is enough to consider the internal induced electric field, namely

$$E_z^{(a)}(\rho,\phi,z,t) = -\frac{\partial \phi_{\rm ind}^{(a)}}{\partial z} = \frac{2}{\pi} Ze \sum_m \int_0^\infty dk\, k I_m(k\rho) I_m(k\rho_0) \times \exp[im(\phi-\phi_0)]\{\mathrm{Re}[\tilde{A}_m(k,\omega)] \times \sin(kz-\omega t) + \mathrm{Im}[\tilde{A}_m(k,\omega)] \times \cos(kz-\omega t)\}\big|_{\omega=kv}. \quad (21)$$

In particular, we may calculate the field acting on the charge (with $z=vt$, $\rho=\rho_0$, and $\phi=\phi_0$), which produces a reaction on it, in the form of a *stopping force* $F_z = ZeE_z^{(a)}$, given by

$$F_z = \frac{2}{\pi}(Ze)^2 \sum_{m=-\infty}^{\infty} \int_0^\infty dk\, k [I_m(k\rho_0)]^2 \mathrm{Im}[\tilde{A}_m(k,\omega)], \quad (22)$$

with $\omega = kv$.

Moreover, since $I_m(x) = I_{-m}(x)$, $K_m(x) = K_{-m}(x)$, the modes with $m>0$ and $m<0$ yield equal contributions and we can write

$$F_z = \sum_{m=-\infty}^{\infty} F_{z,m} = F_{z,0} + 2\sum_{m=1}^{\infty} F_{z,m}, \quad (23)$$

where $F_{z,m}$ is the contribution from each mode m.

Let us consider now some limiting cases of special interest.

A. Limit $ka \to 0$

This limit applies both to the cases of small channel radius or relatively fast particles (i.e., $\omega_s a/v \to 0$), but within the nonrelativistic restrictions.

We use the behavior of the $I_m(x)$ and $K_m(x)$ functions when $x \to 0$, namely[20] $I_m(x) \to a_m x^m$, $I_m'(x) \to m a_m x^{m-1}$, $K_0(x) \to \ln(1.123\ldots/x)$, $K_0'(x) \to -1/x$, $K_m(x) \to b_m x^{-m}$ (for $m \neq 0$), and $K_m'(x) \to -m b_m x^{-(m+1)}$ $(m \neq 0)$, with $a_m = 2^{-m}/\Gamma(m+1)$ and $b_m = 2^{m-1}\Gamma(m)$.

Then we get, for $m=0$,

$$\tilde{A}_0 = K_0(ka)\left[\frac{1-\varepsilon(\omega)}{\varepsilon(\omega)}\right] \cong \ln\left(\frac{1.123}{ka}\right)\left[\frac{1-\varepsilon(\omega)}{\varepsilon(\omega)}\right], \quad (24)$$

and for $m \neq 0$,

$$\tilde{A}_m \cong \frac{b_m}{(ka)^{2m}}\left[\frac{1-\varepsilon(\omega)}{1+\varepsilon(\omega)}\right]. \quad (25)$$

In particular, we can distinguish the following two cases of interest.

1. Motion along the axis ($\rho_0 = 0$)

In this case only the $m=0$ term contributes, yielding a stopping force

$$F_z \cong \frac{2}{\pi}(Ze)^2 \int_0^\infty dk\, k \ln\left(\frac{1.123}{ka}\right) \mathrm{Im}\left[\frac{1}{\varepsilon(\omega)}\right] \quad (26)$$

with $\omega = kv$. Using the dielectric function model, $\varepsilon(\omega) = 1 - \omega_P/\omega(\omega + i\gamma)$, in the limit of small damping ($\gamma \to 0$), $\mathrm{Im}[1/\varepsilon(\omega)] = -(\pi/2)\omega_P[\delta(\omega-\omega_P) - \delta(\omega+\omega_P)]$, we get

$$F_z \cong -\left(\frac{Ze\omega_P}{v}\right)^2 \ln\left(\frac{1.123\, v}{a\omega_P}\right). \quad (27)$$

It is interesting to note that this result agrees with the one corresponding to particles moving uniformly in a homogeneous medium, as it may be expected in the present limit ($\rho_0 = 0$, $a \ll v/\omega_P$) with a cutoff radius given by a.

2. Motion near the axis ($\rho_0 \ll a$)

Using here the limiting forms of the Bessel functions for $x \to 0$, and considering the limit $\mathrm{Im}\{[1-\varepsilon(\omega)]/[1+\varepsilon(\omega)]\} = -(\pi/2)\omega_s[\delta(\omega-\omega_s) - \delta(\omega+\omega_s)]$, with $\omega_s = \omega_P/\sqrt{2}$, we get

$$F_{z,0} \cong -\left(\frac{Ze\omega_P}{v}\right)^2 \ln\left(\frac{1.123\, v}{a\omega_P}\right) \quad (28)$$

and

$$F_{z,m} \cong -\left(\frac{Ze\omega_s}{v}\right)^2 a_m b_m \left(\frac{\rho_0}{a}\right)^{2m} \quad (29)$$

with the values of a_m and b_m given before.

We notice here the quadratic growing of the $m=1$ contribution for small ρ_0, i.e., for particles moving close to the channel axis.

B. Limit $ka \to \infty$

We observe from Eq. (6) that for $x = ka \to \infty$, $g_m(x) \to \frac{1}{2}$ and so $\omega_{k,m} \to \omega_s$; moreover, we obtain in this limit that $k \cong \omega_s/v$. Using these approximations in Eqs. (16) and (22), we get, for $\rho_0 \sim a$,

$$F_z \cong -\left(\frac{Ze\omega_s}{v}\right)^2 \sum_{m=-\infty}^{\infty} I_m(2k\rho_0) K_m(2ka), \quad (30)$$

and using here the property[19]

$$\sum_{m=-\infty}^{\infty} I_m(2k\rho_0) K_m(2ka) = K_0(2k|\rho_0 - a|), \quad (31)$$

we finally obtain

$$F_z \cong -\left(\frac{Ze\omega_s}{v}\right)^2 K_0\left(2\frac{\omega_s}{v}\delta_0\right) \quad (32)$$

with $\delta_0 = |\rho_0 - a|$.

We note that this corresponds to the expression of the stopping force for a particle moving parallel to an infinite *plane* surface,[22] at a distance $\delta_0 = |\rho_0 - a|$. Therefore, in this limit ($ka \to \infty$) the curvature of the surface becomes irrelevant. The interaction decays rapidly for $\delta_0 \omega_s/v \gg 1$, so that it becomes negligible in a wide inside region with $\rho_0 < a$.

Hence, the interaction with the surface occurs only at relatively ''small'' distances, $\delta_0 \sim v/\omega_s$ (with $v/\omega_s \ll a$).

V. CALCULATION OF THE STOPPING FORCE

The expression for the stopping force, Eq. (22), may be integrated in a general way for a dielectric function of the form $\varepsilon(\omega)=\varepsilon_1(\omega)+i\varepsilon_2(\omega)$ when $\varepsilon_2(\omega)\to 0$. As we will see, this provides a more general solution than the one obtained from the simple dielectric model previously used.

First we write the expression for $\tilde{A}_m$ using Eq. (16) as follows:

$$\tilde{A}_m=\frac{X_m}{Y_m+i\varepsilon_2(\omega)Z_m}, \tag{33}$$

where $X_m=[1-\varepsilon(\omega)]K_m(ka)K'_m(ka)$, $Y_m=\varepsilon_1(\omega)I_m(ka)K'_m(ka)-I'_m(ka)K_m(ka)$, and $Z_m=I_m(ka)K'_m(ka)$, which is obtained by separating the real and imaginary parts of $\varepsilon(\omega)=\varepsilon_1(\omega)+i\varepsilon_2(\omega)$ in the denominator of Eq. (16).

Then, for $\varepsilon_2(\omega)\to 0^+$, we use the limiting expression (note that $Z_m<0$)

$$\lim_{\varepsilon_2\to 0^+}\frac{1}{Y_m+i\varepsilon_2 Z_m}\to \mathrm{PV}\left[\frac{1}{Y_m}\right]+i\pi\delta(Y_m). \tag{34}$$

Using this in Eq. (33), we get

$$\mathrm{Im}[\tilde{A}_m]\cong \pi X_m\delta[\varepsilon_1(\omega)I_m(ka)K'_m(ka)-I'_m(ka)K_m(ka)]. \tag{35}$$

Now, since the roots of the square bracket expression are precisely the frequencies of the modes, $\omega_m(k)$ [cf. Eq. (4)], we can also approximate this result as

$$\mathrm{Im}[\tilde{A}_m]\cong -\frac{\pi X_m}{I_m(x)K'_m(x)}\left|\frac{\partial\varepsilon_1}{\partial\omega}\right|^{-1}\{\delta[\omega-\omega_m(k)] - \delta[\omega+\omega_m(k)]\}, \tag{36}$$

where $I_m(x)\equiv I_m(ka)$, $K'_m(x)\equiv K'_m(ka)$, and the value of X_m was given before.

Using this expression in Eq. (22), we obtain the result for the stopping force,

$$F_z=\sum_{-\infty}^{\infty}F_{z,m}, \tag{37}$$

where the contribution of each mode m becomes

$$F_{z,m}=-2\left(\frac{Ze}{v}\right)^2\omega_m\frac{[1-\varepsilon_1(\omega_m)]}{|\partial\varepsilon_1/\partial\omega|}\frac{K_m(ka)}{I_m(ka)}\left[I_m\left(\frac{\omega_m\rho_0}{v}\right)\right]^2. \tag{38}$$

1. Plasma resonance approximation

Let us consider again the approximation for the dielectric function used before, $\varepsilon(\omega)=1-\omega_P^2/\omega(\omega+i\gamma)$, with $\gamma\to 0$. We get $|\partial\varepsilon_1/\partial\omega|=2\omega_P^2/\omega^3$, and Eq. (38) becomes

$$F_{z,m}=-\left(\frac{Ze\omega_m}{v}\right)^2\frac{K_m(ka)}{I_m(ka)}\left[I_m\left(\frac{\omega_m\rho_0}{v}\right)\right]^2. \tag{39}$$

We may write this result in a more illustrative way using the equation for the capillary modes, Eq. (6), $\omega_m^2=\omega_P x I_m(x)|K'_m(x)|$, which yields

$$F_{z,m}=-\left(\frac{Ze\omega_P}{v}\right)^2\left[I_m\left(\frac{\omega_m\rho_0}{v}\right)\right]^2 xK_m(x)|K'_m(x)|, \tag{40}$$

where $x\equiv ka$ and $k=\omega_m/v$. We note here that the dependence on the channel radius is simply parametrized in terms of the function $G_m(x)=xK_m(x)|K'_m(x)|$.

As was already noted, the values of k and ω_m must be determined for each velocity v by solving the intersecting equation $\omega_m(k)=kv$ (condition for resonant excitation of modes), so that the values of k and ω become velocity-dependent functions: $k=k_m[v]$ and $\omega=\omega_m[v]$, as indicated in Sec. III.

VI. QUANTUM-MECHANICAL TREATMENT

In order to quantize the previously described modes of a cylindrical cavity, we will apply the method of surface-plasmon quantization developed in Ref. 2 For this purpose, the energy of the plasmon field is separated into kinetic- and potential-energy terms. The kinetic energy, associated with the electronic oscillations, is represented by introducing a velocity-potential function $\Psi(\mathbf{r},t)$, such that the velocity field corresponding to the electron motion may be calculated as $\mathbf{v}(\mathbf{r},t)=-\boldsymbol{\nabla}\Psi(\mathbf{r},t)$.

The energy of the surface-plasmon field is then given by the sum of potential and kinetic energies as follows:

$$H^0_{sp}=\frac{1}{2}\int\rho_s\phi_s\,d^3r+\tfrac{1}{2}n_0m_e\int(\boldsymbol{\nabla}\Psi)^2d^3r. \tag{41}$$

Here $\rho_s=-en_s$ is the electric charge associated with the induced electronic density n_s of the surface-plasmon field and ϕ_s is the corresponding electrostatic potential, while n_0 is the equilibrium electron density in the metal and m_e is the electron mass.

We write the electrostatic potential as a general expansion including all the modes,

$$\phi_s(\mathbf{r},t)=\sum_{k,m}e^{i(kz+m\varphi)}\begin{cases}\phi^{(1)}_{k,m}(t)I_m(k\rho), & \rho<a\\ \phi^{(2)}_{k,m}(t)K_m(k\rho), & \rho>a\end{cases} \tag{42}$$

and express the electronic density corresponding to these modes as a localized surface density, namely

$$n_s(\mathbf{r},t)=\sum_{k,m}n_{k,m}(t)e^{i(kz+m\varphi)}\delta(\rho-a). \tag{43}$$

The ρ component of the electric field is then derived,

$$\mathbf{E}_\rho\equiv-\frac{\partial\phi_s}{\partial\rho}=-\sum_{k,m}k\,e^{i(kz+m\varphi)}\begin{cases}\phi^{(1)}_{k,m}(t)I'_m(k\rho), & \rho<a\\ \phi^{(2)}_{k,m}(t)K'_m(k\rho), & \rho>a.\end{cases} \tag{44}$$

Finally, we propose an expansion for the velocity-potential field $\Psi(\mathbf{r},t)$ as follows:

$$\Psi(\mathbf{r},t)=\sum_{k,m}\begin{cases}0, & \rho<a\\ \Psi_{k,m}(t)e^{i(kz+m\varphi)}K_m(k\rho), & \rho>a,\end{cases} \quad (45)$$

where we have taken into account the confinement of the electrons to the region $\rho>a$.

In order to determine the relations between the coefficients $\phi_{k,m}$, $n_{k,m}$, and $\Psi_{k,m}$ in these expansions, we apply Maxwell's boundary conditions at $\rho=a$, namely

$$\mathbf{E}_\rho^{(2)}-\mathbf{E}_\rho^{(1)}|_{\rho=a}=-4\pi e\sigma_s, \quad (46)$$

$$\mathbf{E}_\rho^{(1)}-\varepsilon(\omega)\mathbf{E}_\rho^{(2)}|_{\rho=a}=0, \quad (47)$$

where σ_s is the induced surface density associated to the electronic density n_s in Eq. (43), $n_s=\sigma_s\delta(\rho-a)$. To obtain a similar relation for $\Psi(\mathbf{r},t)$, we recall the continuity equation

$$\frac{\partial n_s}{\partial t}=-n_0\nabla\cdot\mathbf{v}=n_0\nabla^2\Psi. \quad (48)$$

By integrating in a small volume containing a small surface element, and using the relation $n_s=\sigma_s\delta(\rho-a)$, we find

$$\left.\frac{\partial\Psi}{\partial\rho}\right|_{\rho=a}=\left.\frac{\dot{\sigma}_s}{n_0}\right|_{\rho=a}, \quad (49)$$

which provides the required link between the fields.

Using Eqs. (46)–(49) and the corresponding expansions in terms of elementary modes, we finally obtain the relations

$$\phi_{k,m}^{(1)}=\frac{4\pi e}{k}\frac{n_{km}}{I_m'(ka)}\frac{\varepsilon(\omega)}{1-\varepsilon(\omega)}, \quad (50)$$

$$\phi_{k,m}^{(2)}=\frac{4\pi e}{k}\frac{n_{km}}{K_m'(ka)}\frac{1}{1-\varepsilon(\omega)}, \quad (51)$$

$$\Psi_{k,m}=\frac{1}{k}\frac{\dot{n}_{km}}{n_0K_m'(ka)}. \quad (52)$$

A. Calculation of energies

Using the expressions (42) and (43), the potential energy in Eq. (41) becomes

$$H_{\rm pot}=-\frac{e}{2}\sum_{k,m}\sum_{k',m'}\int d^3r\, e^{i(k+k')z}e^{i(m+m')\varphi}\times n_{k,m}\phi_{k',m'}^{(1)}I_{m'}(ka)\,\delta(\rho-a), \quad (53)$$

where we separate the volume integral as

$$\int d^3r=\int_0^\infty\rho\,d\rho\int_{-L/2}^{L/2}dz\int_0^{2\pi}d\varphi, \quad (54)$$

and after elementary integrations, and using the relation (50) between $\phi_{-k,-m}^{(1)}$ and $n_{-k,-m}$, we get

$$H_{\rm pot}=-2\pi e^2A\sum_{k,m}\frac{n_{k,m}n_{-k,-m}}{k}\frac{I_m(ka)}{I_m'(ka)}\left(\frac{\varepsilon}{1-\varepsilon}\right), \quad (55)$$

where $A=2\pi La$ is the surface of the cylindrical cavity.

In order to calculate the kinetic energy in Eq. (41), we perform a partial integration as follows:

$$\int d^3r(\nabla\Psi)^2=\int d^2\mathbf{A}\Psi\nabla\Psi-\int d^3r\,\Psi(\nabla^2\Psi). \quad (56)$$

We note that the second term cancels out due to the assumed irrotational property[2] $\nabla^2\Psi=0$, whereas the surface integration is performed using Eq. (45),

$$\int d^2\mathbf{A}\left(\Psi\frac{\partial\Psi}{\partial\rho}\right)=\sum_{k,m}\sum_{k',m'}\int dz\int d\varphi\,\Psi_{k,m}\Psi_{k',m'}\times e^{i(k+k')z}e^{i(m+m')\varphi}\times k'K_m(k\rho)K_{m'}'(k'\rho). \quad (57)$$

Here the z and φ integrals give $\delta_{k',-k}\delta_{m',-m}$, and using Eq. (52) for $\Psi_{k,m}$, we get the kinetic-energy term in the form

$$H_{\rm kin}=-\frac{m_eA}{2n_0}\sum_{k,m}\frac{\dot{n}_{k,m}\dot{n}_{-k,-m}}{k}\frac{K_m(ka)}{K_m'(ka)}. \quad (58)$$

From Eqs. (55) and (58), the total energy of Eq. (41) may be written as

$$H_{\rm sp}^0=2\pi e^2A\sum_{k,m}\frac{n_{k,m}n_{-k,-m}}{k}\alpha_{k,m}+\frac{m_eA}{2n_0}\sum_{k,m}\frac{\dot{n}_{k,m}\dot{n}_{-k,-m}}{k}\beta_{k,m}, \quad (59)$$

where

$$\alpha_{k,m}=\frac{I_m(ka)}{I_m'(ka)}\left(\frac{-\varepsilon}{1-\varepsilon}\right), \quad (60)$$

$$\beta_{k,m}=-\frac{K_m(ka)}{K_m'(ka)}. \quad (61)$$

Using the equation of the modes (4), we obtain

$$\alpha_{k,m}=\frac{\beta_{k,m}}{1-\varepsilon}=\beta_{k,m}\frac{\omega_{k.m}^2}{\omega_P^2}, \quad (62)$$

where the last expression applies to the dielectric function $\varepsilon(\omega)=1-\omega_P^2/\omega(\omega+i\gamma)$ considered before.

It may also be proved that $\alpha_{k,m}$ and $\beta_{k,m}$ are always positive quantities, since by Eq. (4) $\varepsilon(\omega)$ should be negative at the frequencies of the surface-plasmon modes.

Using Eq. (4) in Eq. (59), we finally obtain the energy of the plasmon field in the desired canonical form,

$$H^0_{\rm sp}=\frac{m_e A}{2n_0}\sum_{k,m}\frac{\beta_{k,m}}{k}[\dot{n}_{k,m}\dot{n}^*_{k,m}+\omega^2_{k.m}n_{k,m}n^*_{k,m}], \quad (63)$$

where the relations $n_{-k,-m}=n^*_{k,m}$ and $\dot{n}_{-k,-m}=\dot{n}^*_{k,m}$ have been used.

B. Quantization

The expression (63) suggests a quantization via a canonical transformation,

$$n_{k,m}=\frac{\gamma_{k,m}}{2\omega_{k,m}}(a_{k,m}+a^*_{-k,-m}),$$
$$n^*_{k,m}=\frac{\gamma_{k,m}}{2\omega_{k,m}}(a^*_{k,m}+a_{-k,-m}), \quad (64)$$

and the corresponding relations (using $\dot{a}_{k,m}=-i\omega_{k.m}a_{k,m}$, $\dot{a}^*_{k,m}=i\omega_{k.m}a^*_{k,m}$)

$$\dot{n}_{k,m}=-\frac{i\gamma_{k,m}}{2}(a_{k,m}-a^*_{-k,-m}),$$
$$\dot{n}^*_{k,m}=\frac{i\gamma_{k,m}}{2}(a^*_{k,m}-a_{-k,-m}). \quad (65)$$

This brings Eq. (63) into the form

$$H^0_{\rm sp}=\frac{m_e A}{4n_0}\sum_{k,m}\frac{\beta_{k,m}}{k}\gamma^2_{k,m}[a_{k,m}a^*_{k,m}+a^*_{k,m}a_{k,m}], \quad (66)$$

so that, with the appropriate choice of $\gamma_{k,m}$,

$$\gamma_{k,m}=\left[\frac{2n_0\hbar k}{m_e A}\frac{\omega_{k,m}}{\beta_{k,m}}\right]^{1/2}, \quad (67)$$

we obtain

$$H^0_{\rm sp}=\tfrac{1}{2}\sum_{k,m}\hbar\omega_{k,m}[a_{k,m}a^*_{k,m}+a^*_{k,m}a_{k,m}]. \quad (68)$$

The quantization may now be performed through the substitution

$$a_{k,m},a^*_{k,m}\rightarrow a_{k,m},a^\dagger_{k,m}, \quad (69)$$

where $a_{k,m},a^\dagger_{k,m}$ are now the operators of annihilation and creation of surface plasmons for each mode k,m, satisfying the usual commutation relations of bosonic operators, their time evolution being of the form $e^{-i\omega t}$ and $e^{i\omega t}$, respectively.[23]

Using these relations, we finally get the expression for the Hamiltonian of the surface-plasmon field in the standard form,

$$H^0_{\rm sp}=\sum_{k,m}\hbar\omega_{k,m}[a^\dagger_{k,m}a_{k,m}+\tfrac{1}{2}]. \quad (70)$$

The eigenstates of $H^0_{\rm sp}$ may be built starting from the vacuum state $|0\rangle$ in the usual way,

$$|n_{k,m}\rangle=\frac{(a^\dagger_{k,m})^n}{\sqrt{n!}}|0\rangle, \quad (71)$$

corresponding to the excitation of $n_{k,m}$ plasmons in a given mode k,m.

VII. INTERACTION WITH EXTERNAL PROBES

Starting from the classical description, the interaction of the plasmon field with an external particle of charge Ze moving along a prescribed trajectory $\vec{r}(t)$ is given by

$$H_{\rm int}=Ze\phi_s[\vec{r}(t)], \quad (72)$$

where ϕ_s is given by Eq. (42).

For particles moving within the channel, we use the first form of Eq. (42) in terms of $\phi^{(1)}_{k,m}$. Moreover, using the relation (50) between the coefficients $\phi^{(1)}_{k,m}$ and $n_{k,m}$ and the relation (64), we can write $\phi^{(1)}_{k,m}$ in terms of the operators a and $a^\dagger$ as follows:

$$\phi^{(1)}_{k,m}=-\lambda_{k,m}(a_{k,m}+a^\dagger_{-k,-m}), \quad (73)$$

where

$$\lambda_{k,m}=\frac{2\pi e}{k}\frac{\omega_{k,m}}{\omega^2_P}\frac{\beta_{k,m}\gamma_{k,m}}{I_m(ka)}. \quad (74)$$

Thus we obtain the expansion of the plasmon field in terms of creation and annihilation operators and the corresponding (internal) eigenfunctions $I_m(k\rho)$ for each mode, in the form

$$\phi_s(\rho<a)=-\sum_{k,m}\lambda_{k,m}I_m(k\rho)(a_{k,m}e^{i(kz+m\varphi)}+a^\dagger_{k,m}e^{-i(kz+m\varphi)}). \quad (75)$$

Using this in Eq. (72), we obtain the expression for the interaction energy for particles moving inside the cavity along a trajectory $\vec{r}(t)$,

$$H_{\rm int}(t)=-Ze\sum_{k,m}\lambda_{k,m}I_m(k\rho)(a_{k,m}e^{i(kz+m\varphi)}+a^\dagger_{k,m}e^{-i(kz+m\varphi)})\big|_{\vec{r}=\vec{r}(t)}, \quad (76)$$

where now the values of (ρ,φ,z) are those corresponding to the trajectory $\vec{r}(t)$.

The values of the coupling coefficients $\lambda_{k,m}$ in this equation may be further simplified using the expressions for $\beta_{k,m}$ and $\gamma_{k,m}$, as well as the equation for the modes, Eq. (6), yielding a very compact result:

$$\lambda^2_{k,m}=\frac{\hbar\omega_{k,m}}{L}\frac{K_m(ka)}{I_m(ka)}. \quad (77)$$

VIII. EXCITATION OF MODES

The total Hamiltonian for the plasmon field interacting with an external probe is given now in the second-quantization formalism by

$$H = H_{\rm sp}^0 + H_{\rm int}(t), \tag{78}$$

where $H_{\rm sp}^0$ and $H_{\rm int}(t)$ are given by Eqs. (70) and (76), respectively. We note that $H_{\rm int}(t)$ may be written as

$$H_{\rm int}(t) = -Ze\sum_{k,m}\,[a_{k,m}f_{k,m}(t) + a_{k,m}^{\dagger}f_{k,m}^{*}(t)], \tag{79}$$

with $f_{k,m}(t) = \lambda_{k,m} I_m(k\rho) e^{i(kz+m\varphi)}$.

Due to the special form of the interaction Hamiltonian, the problem of determining the evolution of this system may be solved in an exact quantum-mechanical way[3] from the Schrödinger equation,

$$i\hbar\,\frac{\partial|\Psi(t)\rangle}{\partial t} = H_{\rm int}|\Psi(t)\rangle, \tag{80}$$

where $|\Psi(t)\rangle$ denotes the quantum state of the plasmon field in the interaction picture.

This problem is formally equivalent to the interaction of charged particles with a flat surface, and it is known that the state of the field is represented as a *coherent state*[23] having the general form[6]

$$|\Psi(t)\rangle = \exp\left[-i\sum_{\mathbf{q}}\,X_{\mathbf{q}}(t)a_{\mathbf{q}} + X_{\mathbf{q}}^{*}(t)a_{\mathbf{q}}^{\dagger}\right]|\Psi(-\infty)\rangle, \tag{81}$$

with

$$X_{\mathbf{q}}(t) = -\frac{Ze}{\hbar}\int_{-\infty}^{t} f_{\mathbf{q}}(t')\exp(-i\omega_{\mathbf{q}}t')\,dt', \tag{82}$$

where for simplicity we are using the condensed notation $\mathbf{q} = (k,m)$ for the modes.

Expanding the solution of Eq. (81) in eigenstates $|n_{\mathbf{q}}\rangle$ of the free Hamiltonian $H_{\rm sp}^0$, Eqs. (70) and (71), we obtain

$$|\Psi(t)\rangle = \prod_{\mathbf{q}}\,\exp(-\tfrac{1}{2}|X_{\mathbf{q}}(t)|^2)\sum_{n=0}^{\infty}\,[-iX_{\mathbf{q}}^{*}(t)]^n\frac{(a_{\mathbf{q}}^{\dagger})^n}{n!}|0\rangle, \tag{83}$$

which contains the complete time evolution of the plasmon field.

A. Probability distributions

From Eq. (83) we can now calculate the probability of excitation of n plasmons of a given state $\mathbf{q}$,

$$P_{n_{\mathbf{q}}}(t) = |\langle n_{\mathbf{q}}|\Psi(t)\rangle|^2 = \exp(-Q_{\mathbf{q}})\frac{(Q_{\mathbf{q}})^n}{n!}, \tag{84}$$

where $Q_{\mathbf{q}} = |X_{\mathbf{q}}(t)|^2$.

More generally, the probability of exciting $n_{\mathbf{q1}}$ plasmons in mode $\mathbf{q}_1$, $n_{\mathbf{q2}}$ plasmons in mode $\mathbf{q}_2$, and so on, will be given by

$$P_{\{n_{\mathbf{q}}\}}(t) = |\langle n_{\mathbf{q1}}, n_{\mathbf{q2}}, \ldots|\Psi(t)\rangle|^2 = e^{-Q_{\mathbf{q1}}}\frac{(Q_{\mathbf{q1}})^{n_{\mathbf{q1}}}}{n_{\mathbf{q1}}!}e^{-Q_{\mathbf{q2}}}\frac{(Q_{\mathbf{q2}})^{n_{\mathbf{q2}}}}{n_{\mathbf{q2}}!}\cdots, \tag{85}$$

which may also be written as

$$P_{\{n_{\mathbf{q}}\}}(t) = e^{-Q}\prod_{\mathbf{q}}\,\frac{(Q_{\mathbf{q}})^{n_{\mathbf{q}}}}{n_{\mathbf{q}}!}, \tag{86}$$

where $Q = \Sigma_{\mathbf{q}}Q_{\mathbf{q}} = \Sigma_{k,m}|X_{k,m}|^2$.

Alternatively, one may be interested in the excitation of a given mode m, so that the appropriate Q value for this case becomes

$$Q_m = \sum_{k}\,|X_{k,m}|^2 = \left(\frac{L}{2\pi}\right)\int_{-\infty}^{\infty} dk|X_{k,m}|^2, \tag{87}$$

where the sum has been transformed into an integral over k following the standard procedure. Note that here the integral extends from $-\infty$ to $+\infty$, whereas in the classical calculation it is restricted to positive k values; this difference is due to the different representations used in each case (here we are using an extended representation in terms of e^{ikz} functions with positive and negative values of k).

These Q values are the parameters of the Poisson distributions describing the probabilities of multiplasmon processes, according to the following.

(a) The probability of exciting a total number N of plasmons in any mode (i.e., $n_{\mathbf{q1}} + n_{\mathbf{q2}} + \cdots = N$) is given by

$$P_N(t) = \sum_{n_{\mathbf{q1}}+n_{\mathbf{q2}}+\cdots=N} P_{\{n_{\mathbf{q}}\}}(t) = e^{-Q}\frac{(Q)^N}{N!}. \tag{88}$$

(b) The probability of exciting N_m plasmons of a given mode m is given by

$$P_{N_m}(t) = e^{-Q_m}\frac{(Q_m)^{N_m}}{N_m!}. \tag{89}$$

The Q values also have the following physical interpretation.

(i) The average total number $\overline{N}$ of excited plasmons is given by $\overline{N} = \Sigma_{N=0}^{\infty} N\,P_N = Q$.

(ii) The average number $\overline{N_m}$ of excited plasmons of mode m is given by $\overline{N_m} = \Sigma_{N_m=0}^{\infty} N_m\,P_{N_m} = Q_m$.

B. Calculation of Q_m

The values of Q_m may be obtained from Eqs. (82) and (87), and using the expressions for the $f_{k,m}$ functions in Eq. (79), namely $f_{k,m}(t) = \lambda_{k,m} I_m(k\rho) e^{i(kz+m\varphi)}$. To integrate $X_{\mathbf{q}}$ (with $\mathbf{q} = k,m$) in Eq. (82), we have to specify the trajectory $(\rho(t), \varphi(t), z(t))$ of the particle. We will now perform the calculation for a trajectory parallel to the axis of the channel with $\rho = \rho_0$, $\varphi = \varphi_0$, $z = vt$ in order to compare with the classical calculation. In this case, since the interaction with

the surface is permanently connected, to avoid divergencies we have to limit our integration to a finite time interval: $-T<t<T$, so that

$$X_{k,m}=-\frac{Ze}{\hbar}\int_{-T}^{T} f_{k,m}(t)\exp(-i\omega_{k,m}t)dt, \tag{90}$$

which yields

$$X_{k,m}=-\frac{Ze}{\hbar}\lambda_{k,m}I_m(k\rho_0)e^{im\varphi_0}\left[\frac{e^{i\Omega T}-e^{-i\Omega T}}{i\Omega}\right] \tag{91}$$

with $\Omega=kv-\omega_m(k)$ [and with $\omega_m(k)\equiv\omega_{k,m}$].

Considering now the limit $T\to\infty$, and using the δ-function limit $[\sin(\Omega T)/\Omega]^2\to\pi T\delta(\Omega)$, we get

$$|X_{k,m}|^2=\frac{4\pi T}{\hbar^2}[Ze\lambda_{k,m}I_m(k\rho_0)]^2\delta(kv-\omega_m(k)). \tag{92}$$

Using Eq. (87) and performing the k integration, we finally obtain

$$Q_m=\frac{2TL}{\hbar^2 v}[Ze\lambda_{k,m}I_m(k\rho_0)]^2. \tag{93}$$

As was already discussed, the value of k is fixed for each mode m and ion velocity v by the resonant condition $\omega_m(k)=kv$ as illustrated in Fig. 1 (line $\omega=ux$). Hence, the value of $\lambda_{k,m}$ to be used in the calculations, Eq. (77), becomes also a velocity-dependent coefficient.

We finally note that the result for Q_m, Eq. (93), is proportional to the interaction time $2T$, which we may replace by L/v (L being the length of the channel), so that the first factor in Q_m is proportional to L^2; but there is an additional factor $1/L$ in the coefficient $\lambda_{k,m}^2$ [cf. Eqs. (67), (74), and (77)], so that the final result for Q_m will be strictly proportional to L.

C. Correspondence with the classical description

There is apparently little similitude between the result obtained for Q_m, Eq. (93), and the previous result for the stopping force obtained from the classical calculation, Eq. (40). However, since there is a correspondence between the dielectric function used in Sec. III and the description of surface plasmons applied in Sec. VI,[3,4] one may expect that there should be a direct connection between both results.

In order to derive this relation, we substitute the value of $\lambda_{k,m}$ in Eq. (93) and the corresponding values of $\beta_{k,m}$ and $\gamma_{k,m}$ using Eqs. (61), (67), and (77), obtaining after some algebra

$$Q_m=\frac{L}{a}\frac{(Ze)^2}{\hbar v}\left(\frac{\omega_{k,m}}{\omega_P}\right)^2\frac{K_m(ka)}{|K_m'(ka)|}\left[\frac{I_m(k\rho_0)}{I_m(ka)}\right]^2. \tag{94}$$

Moreover, using Eq. (6) for the frequency of the modes, we may cast the result in the following form:

$$Q_m=\frac{L}{\hbar\omega_m}\left(\frac{Ze\omega_P}{v}\right)^2 xK_m(x)|K_m'(x)|[I_m(k\rho_0)]^2. \tag{95}$$

It should be noted that in these expressions the value of k is fixed as ω_m/v, and so $x=ka=\omega_m a/v$ (see also the next section for further discussion).

By comparing with Eq. (40), we obtain the desired connection between both formalisms:

$$L|F_{z,m}|=\hbar\omega_m Q_m, \tag{96}$$

which yields the *average* energy loss due to excitations of each type of surface mode m.

In addition, the average energy loss ΔE of the particle after traversing a distance L inside the channel may be calculated following either of the two formalisms, yielding also coincident results

$$\Delta E=-L\sum_{-\infty}^{\infty}F_{z,m}=\sum_{-\infty}^{\infty}\hbar\omega_m Q_m. \tag{97}$$

These relations are in full agreement with the interpretation of Q_m as giving the average number of plasmons being excited on each mode, with corresponding energy $\hbar\omega_m$. In this way, previous calculations based on the classical formalism[9–11] convey also information on surface-plasmon excitation.

IX. SCALING PROPERTIES

It was already noted in Sec. II that $\omega_{k,m}/\omega_P$ is determined in a general way by a function (or set of functions) of the variable $x=ka$, namely $\omega_{k,m}/\omega_P=\sqrt{g_m(x)}$, with $g_m(x)\equiv xI_m(x)|K_m'(x)|$, Eq. (6). On the other hand, in the integration of the induced potential, electric field, and stopping force—Eqs. (18), (21), and (22)—the phase-matching condition $\omega_m(k)=kv$ was imposed. Then, we may express this condition as $\sqrt{g_m(x)}=kv/\omega_P=xv/a\omega_P$, or simply

$$\sqrt{g_m(x)}=ux, \tag{98}$$

where we introduce the *reduced velocity*

$$u=\frac{v}{a\omega_P}. \tag{99}$$

The condition (98) was illustrated in Fig. 1, and corresponds to the intersection of the line ux with the curves $\omega_{k,m}/\omega_P=\sqrt{g_m(x)}$. Thus, for each reduced velocity u there is a unique set of values of the variable x for each mode m, $x_m=x_m(u)$, which determine the values of $k=k_m(u)=x_m(u)/a$ and of $\omega=\omega_m(u)$. By varying the velocity v (or u), these values change in a continuous way. The functions $x_m(u)$ are shown in Fig. 2; as it may be observed, for large values of u the simple relations $x_0(u)\sim 1/u$ and $x_m(u)\sim 1/\sqrt{2}u$ (for $m\neq 0$) may be applied, whereas for $u\ll 1$, $x_m(u)$ may be approximated by $x_m(u)\sim 1/\sqrt{2}u$ for all m values.

Using these properties, the expression for the stopping force of Eq. (40) may be parametrized as follows:

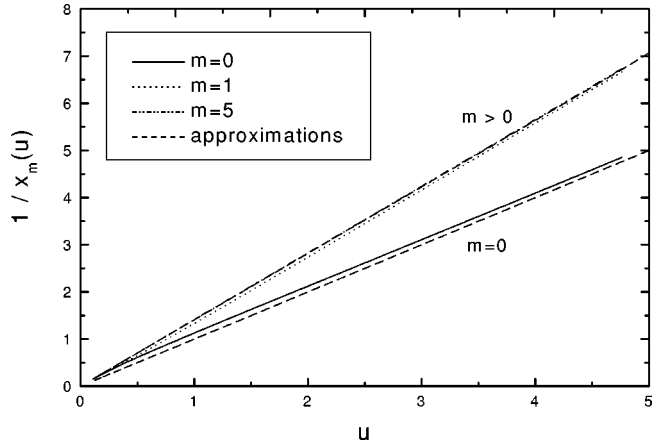

FIG. 2. Functions $1/x_m(u)$ for the modes with $m=0,1,5$. The values of $x_m(u)$ are those corresponding to the intersection points with the line $\omega/\omega_P = ux$ indicated in Fig. 1 The dashed lines show the approximations $x_0(u) \sim 1/u$ and $x_m(u) \sim 1/\sqrt{2}u$ (for all $m \neq 0$), which apply for large values of u.

$$F_{z,m} = -\left(\frac{Ze\omega_P}{v}\right)^2 xK_m(x)|K_m'(x)|[I_m(x\xi)]^2, \quad (100)$$

in terms of the variable $x=ka$ defined before and introducing also the reduced variable

$$\xi = \frac{\rho_0}{a}. \quad (101)$$

Replacing $v = ua\omega_P$ in Eq. (100), we may also write

$$F_{z,m} = -\frac{E_a}{a} f_m(u,\xi). \quad (102)$$

Here $E_a = (Ze)^2/a$ is a typical value of energy for this system, whereas the functions

$$f_m(u,\xi) = \frac{1}{u^2} xK_m(x)|K_m'(x)|[I_m(x\xi)]^2\Big|_{x=x_m(u)}. \quad (103)$$

may be considered universal functions of the independent variables $u = v/a\omega_P$ and $\xi = \rho_0/a$, due to the fact that $x = x_m(u)$ is a function of u. This way of scaling the results in terms of (u,ξ) becomes more advantageous than the previous one in terms of (x,ξ) since it shows the velocity dependence in a direct way.

The functions $f_m(u,\xi)$ are shown in Fig. 3 for $m=0$, 1, and 2. The main features of these results are the existence of maxima for intermediate values of u, except for the case $\xi = 1$ (or $\rho_0 = a$), where the curves show no maximum, and a general increase of the values with increasing ξ, i.e., as the particle approaches the boundary of the capillary. The lower values of f_m occur always for $\xi = 0$ (on the channel axis) where the only nonvanishing term is given by the lowest mode with $m=0$. As a reference, the maximum value of the $m=0$ function for the case of particles channeled along the axis, $f_0(u,0)$, is found at $u_{\max} = 0.8$, Fig. 3(a). Due to the

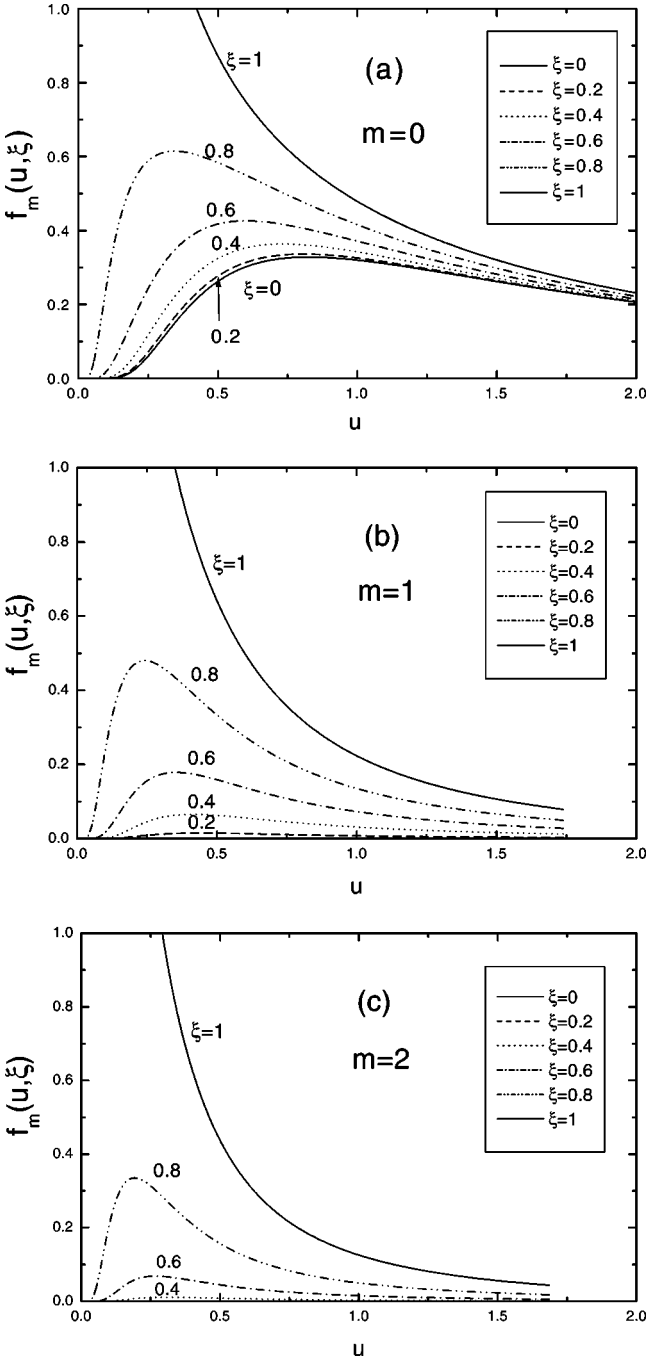

FIG. 3. General functions $f_m(u,\xi)$ (where $u = v/\omega_P a$ and $\xi = \rho_0/a$) for the cases (a) $m=0$, (b) $m=1$, and (c) $m=2$. The curves for $\xi=0$ correspond to particles moving along the channel axis, whereas $\xi=1$ correspond to trajectories touching the cavity radius ($\rho_0 = a$).

relation between u and v, this shows that the maximum value of the stopping force or related quantities for this case will occur for particle velocities proportional to the channel radius, namely $v_{\max} = 0.8\omega_P a$.

The previous analysis may also be applied to the Q_m values required for the description of surface-plasmon excitations. These values may be calculated from the f_m functions as follows:

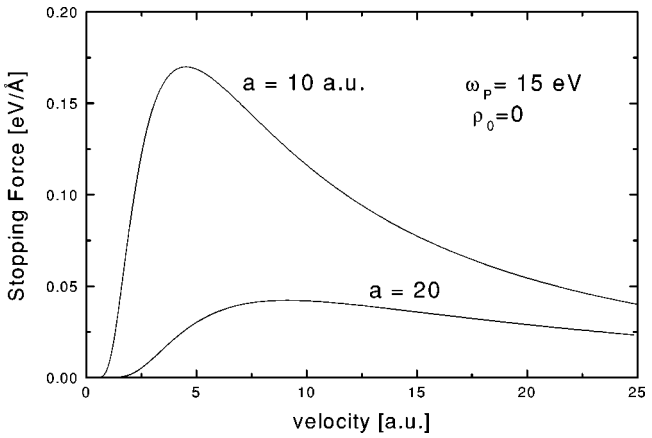

FIG. 4. Calculation of the stopping force (or stopping power), according to Eqs. (100) and (103), vs the particle velocity, for channels with radii $a=10$ and $a=20$ a.u., for a medium with plasma frequency $\omega_P=0.55$ a.u. The shift in the curves follows from the scaling properties contained in Eq. (102). In particular, the maximum stopping value decreases with $1/a^2$ while the position of the maximum grows linearly with a.

$$Q_m=\frac{L}{\hbar\omega_m}|F_{z,m}|=\frac{E_a}{\hbar\omega_m}\frac{L}{a}f_m(u,\xi). \tag{104}$$

In the next section, we will give some examples illustrating these results.

X. CALCULATIONS

Here we consider some examples of the results derived before. For simplicity, we will assume an incident particle with unit charge, $Z=1$ (e.g., a proton or electron). For other Z values (as for multicharged ions), one could use the quadratic (Z^2) scaling of the stopping force or other linearly related quantities. However, one should note that the values of the probabilities of plasmon excitation P_n do not satisfy the Z^2 scaling, and so they should be recalculated for other Z values.

In Fig. 4, we show a calculation of the stopping force (or stopping power), Eqs. (100) and (102), versus the particle velocity, for channels with radii $a=10$ and $a=20$ a.u., for a medium with plasma frequency $\omega_P=0.55$ a.u. The maximum stopping values decrease with $1/a^2$ while the position of the maximum grows linearly with a as indicated before. As observed, these stopping power values should lead to energy losses of the order of hundreds of eV if the lengths of the channels are of some thousands of Å . The observation of multiple plasmon-loss peaks in these cases should be expected (note by comparison that only single plasmon peaks with small intensities have been observed in experiments with larger capillary radii).[7,8]

The dependence of the stopping force with the ρ_0 value is indicated in Fig. 5, for the case $a=10$ a.u. Here we include the contribution of the terms with $m=0,1,\ldots,5$. We observe the dominance of the $m=0$ term near the axis and up to $\rho_0\sim a/2$, whereas when $\rho_0\to a$ the result approaches the analytical value predicted by Eq. (32).

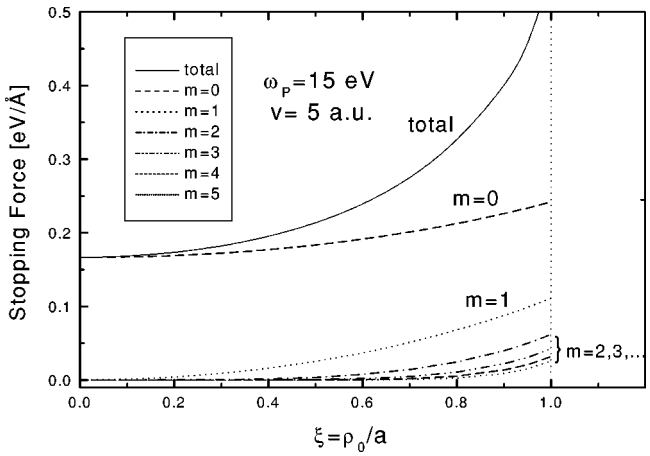

FIG. 5. Stopping force on the particle as a function of ρ_0 for the case $a=10$ a.u. The contribution of the terms with $m=0,1,\ldots,5$ is indicated. The $m=0$ term yields the only contribution near the channel axis, $\rho_0\to 0$, whereas for $\rho_0\to a$ the stopping force approaches the value for flat surfaces predicted by Eq. (32).

Let us consider now the calculation of plasmon-excitation processes. In Fig. 6, we show the Q_m values, for $m=0,1,2$, for a proton traveling with $\rho_0=0.5a$ in a channel with $a=10$ and $L=1000$ a.u., whereas in Fig. 7, we show the corresponding probabilities P_n of exciting a number n of plasmons in the mode $m=0$, with $0\leqslant n\leqslant 5$, calculated according to Eq. (89). The velocity dependence of probabilities P_n may be analyzed in further detail considering the correspondence with the Q_m values shown in Fig. 6. Thus, for instance, at $v=10$ we find in Fig. 7 a maximum probability of exciting $n=4$ plasmons, whereas at $v=20$ the maximum probability is for $n=2$ plasmons; these values are in agreement with the values of $Q_{m=0}$ for $v=10$ and $v=20$ in Fig. 6 On the other hand, in the high-velocity limit (where the Q values drop to 0), we observe a maximum probability of the no-plasmon excitation process (the elastic channel).

The probabilities P_n also have an important dependence on the channel length L. In Fig. 8, we show this dependence

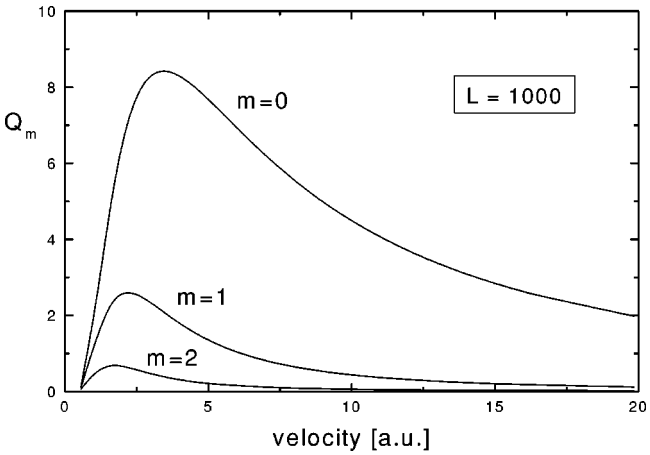

FIG. 6. Calculation of Q_m, with $m=0,1,2$, for a proton traveling with impact parameter $\rho_0=0.5a$ in a channel with radius $a=10$ a.u. and length $L=1000$ a.u.

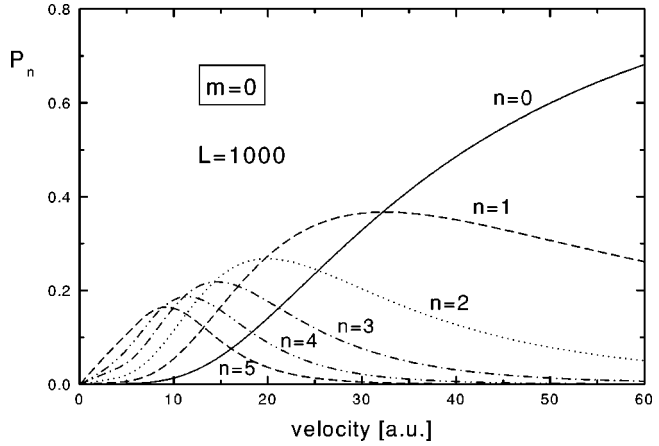

FIG. 7. Probabilities P_n of exciting n plasmons (with $0 \leqslant n \leqslant 5$) in mode $m=0$, after traversing a fixed distance L, as a function of velocity, calculated according to Eq. (89) and for the case of Fig. 6 ($\rho_0 = 0.5a$, $a=10$, $L=1000$).

considering also $a=10$ and assuming now a fixed velocity $v=5.5$ a.u. The figure shows the exponential decrease of the elastic peak and the increase of the $n=1,2,\ldots$ processes with increasing L. This may be explained rather simply from the linear increase of Q_m with L, Eq. (95), and consistently with the values of Q_m shown in Fig. 6 and with the interpretation of Q_m as the average number of plasmon excitations expected for a given length L.

We finally indicate that the present values have been produced only for illustrative purposes, and the parameters used here are in the range of interest for experiments with small-size nanotubes.[12–15] Much larger values of a and L would be of interest for other experiments with microcapillaries in metals.[7,8,18]

With respect to the applicability of the present results to materials having more complicated dielectric properties than the simple plasma resonance model used here, we can note that the semiclassical approach and the general results derived in Secs. III and IV [such as Eqs. (21)–(23), as well as expression (16) for $\tilde{A}_m(k,\omega)$] may be applied in principle to any dielectric function. These results could then be used to calculate multiple-energy-loss spectra of experimental interest through convolution methods such as those discussed in Refs. 24 and 25

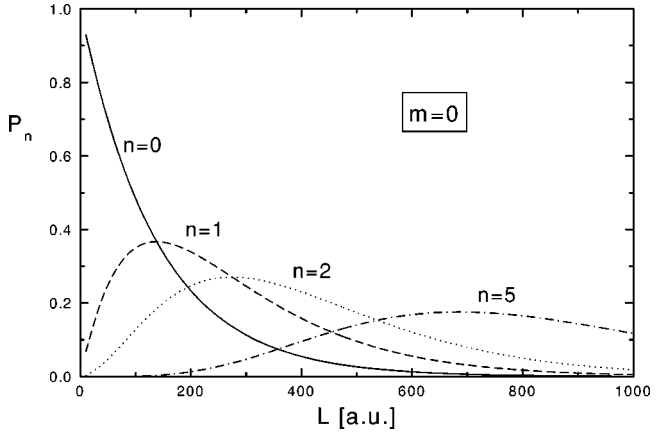

FIG. 8. Probabilities P_n of exciting n plasmons (with $0 \leqslant n \leqslant 5$) in mode $m=0$, as a function of the traversed distance L, for a fixed velocity $v=5.5$ a.u. (with $\rho_0 = 0.5a$ and $a=10$).

XI. SUMMARY

We have studied the interaction of charged particles with surface modes in cylindrical cavities using both classical and quantum-mechanical formulations. The classical description follows the lines of previous approaches, providing a simplified and useful view of the process, and obtaining several new results. The quantization of the surface-plasmon modes has been carried out, deriving from first principles the form of the Hamiltonian that describes the interaction with external probes.

The excitation of these modes by charged particles has been studied in detail, and general scaling properties have been obtained. This provides a set of scaling functions that may be useful to predict energy losses and plasmon excitation probabilities in many cases of practical interest. The application of the general results has been illustrated by numerical examples for particle velocities and cavity sizes in the range of experimental access.

ACKNOWLEDGMENTS

This work was supported in part by CONICET and ANPCYT of Argentina (PICT0303579). M.A.F. wishes to acknowledge support from the ANPCYT.

[1] R. H. Ritchie, Phys. Rev. **106**, 874 (1957).
[2] R. H. Ritchie and R. E. Wilems, Phys. Rev. **178**, 372 (1969).
[3] A. A. Lucas and M. Šunjić, Prog. Surf. Sci. **1**, 75 (1972); A. A. Lucas, Phys. Rev. B **20**, 4990 (1979).
[4] G. D. . Mahan, Phys. Status Solidi B **55**, 703 (1973).
[5] C. J. Powell, Phys. Rev. **175**, 972 (1968).
[6] C. Denton, J. L. Gervasoni, R. O. Barrachina, and N. R. Arista, Phys. Rev. A **57**, 4498 (1998).
[7] R. J. Warmack, R. S. Becker, V. E. Anderson, R. H. Ritchie, Y. T. Chu, J. Little, and T. L. Ferrell, Phys. Rev. B **29**, 4375 (1984).
[8] K. C. Mamola, R. J. Warmack, and T. L. Ferrell, Phys. Rev. B **35**, 2682 (1987).
[9] Y. T. Chu, R. J. Warmack, R. H. Ritchie, J. Little, R. S. Becker, and T. L. Ferrell, Part. Accel. **16**, 13 (1984).
[10] M. Schmeits, Solid State Commun. **67**, 169 (1988).
[11] N. Zabala, A. Rivacoba, and P. M. Echenique, Surf. Sci. **209**, 465 (1989).
[12] S. Iijima, Nature (London) **354**, 56 (1991); **356**, 776 (1992).
[13] T. W. Ebbesen and P. M. Ajayan, Nature (London) **358**, 220 (1992).
[14] V. P. Dravid *et al.*, Science **259**, 1601 (1993).

[15] L. A. Gevorgyan, K. A. Ispiryan, and R. K. Ispiryan, Pis'ma Zh. Éksp. Teor. Fiz. **66**, 304 (1997) [JETP Lett. **66**, 322 (1997)]; Nucl. Instrum. Methods Phys. Res. B **145**, 155 (1998).
[16] A. Thess *et al.*, Science **273**, 483 (1996).
[17] S. Ninomiya, Y. Yamazaki, F. Koike, H. Masuda, T. Azuma, K. Komaki, K. Kuroki, and M. Sekiguchi, J. Phys. Soc. Jpn. **65**, 1199 (1996); Phys. Rev. Lett. **78**, 4557 (1997).
[18] K. Tőkési, L. Wirtz, and J. Burgdörfer, Nucl. Instrum. Methods Phys. Res. B **154**, 307 (1999); K. Tőkési, L. Wirtz, C. Lemell, and J. Burgdörfer, *ibid.* **164-165**, 504 (2000).
[19] J. D. Jackson, *Classical Electrodynamics* (Wiley, New York, 1975).
[20] M. Abramowitz and I. A. Stegun, *Handbook of Mathematical Functions* (Dover, New York, 1972).
[21] P. M. Echenique, R. H. Ritchie, and W. Brandt, Phys. Rev. B **20**, 2567 (1979).
[22] P. M. Echenique and A. Howie, Ultramicroscopy **16**, 269 (1985); N. R. Arista, Phys. Rev. A **49**, 1885 (1994).
[23] E. Merzbacher, *Quantum Mechanics* (Wiley, New York, 1970).
[24] J. Daniels, C. V. Festenberg, H. Raether, and K. Zeppenfeld, in *Optical Constants of Solids by Electron Spectroscopy*, edited by G. Höhler, *Springer Tracts in Modern Physics* Vol. 54 (Springer, Berlin, 1970), p. 77.
[25] Ph. Lambin, J. P. Vigneron, and A. A. Lucas, Phys. Rev. B **32**, 8203 (1985).